

Mutant p53 and ELK-1 co-drive the expression of FRA-1 in breast cancer cells

Sike Hu (✉ husike@126.com)

Tianjin Institute of Medical & Pharmaceutical Sciences

Manxue Wang

Tianjin Institute of Medical & Pharmaceutical Sciences

Ailing Ji

Tianjin Medicine and Health Research Center

Jie Yang

Tianjin Medicine and Health Research Center

Ruifang Gao

Tianjin Institute of Medical & Pharmaceutical Sciences

Xia Li

Tianjin Institute of Medical & Pharmaceutical Sciences

Lili Sun

Tianjin Medicine and Health Research Center

Zibo Yang

Tianjin Institute of Medical & Pharmaceutical Sciences

Ying Zhang

Tianjin Medicine and Health Research Center

Hongbin Liu

Tianjin Medicine and Health Research Center

Article

Keywords:

Posted Date: March 17th, 2022

DOI: <https://doi.org/10.21203/rs.3.rs-1452900/v1>

License: © ⓘ This work is licensed under a Creative Commons Attribution 4.0 International License.

[Read Full License](#)

Abstract

Tumor-related p53 mutations can provoke activities different from p53 wild-type tumors to lose tumor-suppressing function. Cells harboring p53 mutations possess a more aggressive property associated with highly pro-invasion, pro-metastasis, proliferation, and cell survival. By comparing the gene expression profiles of p53 mutant and p53 knockdown cancer cells, we figure out FRA-1 as a potential effector of mtp53-mediated metastasis. We demonstrate that the expression of FRA-1, a gatekeeper of mesenchymal-epithelial transition encoded by FOSL1, elevates in the presence of p53 mutations. Mechanistically, mutant p53 binds to ELK-1 in BRCA cells, implying their collaboration to induce FRA-1 expression. In short, this study deciphers new insights into how mtp53 handles metastasis.

Introduction

TP53 in its wild-type form exerts a suppressive function in tumors. Wild-type p53 is involved in cellular senescence, cell cycle arrest, genome maintenance, apoptosis, and DNA repair in the active state. TP53 mutation is the leading cause of human cancer cells¹. The general genetic alterations of p53 compromise the activity of wild-type p53, which is called loss of function (LOF)². And it exerts a dominant-negative (DN) function against the remaining wild-type p53. In addition, there is increasing evidence that mounts p53 mutants exhibit gain-of-function (GOF) characteristics, by which mtp53 possesses "carcinogenic" properties and leads to a more aggressive tumor phenotype³.

Mutant p53 (mtp53) is an effective metastasis regulator. Much evidence proves that mtp53 leads to the roughly similar acquisition of invasive and metastatic activities. To destruct epithelial polarity and reduce the integrity of cell-cell connections, mtp53 favors EMT programs by upregulating specific TFs such as ZEB1, ZEB2, SNAIL, SLUG⁴⁻⁶. Besides, several RTK pathways such as EGFR, AKT, PDGFR β , and HGF/MET were induced by mutant p53 to promote tumor invasion and metastasis⁷. Mtp53 plays a vital role in the spatial regulation of RhoA activity by inducing MYO10. By harnessing the endocytic recycling machinery, mtp53 enhances the transport of integrin to the plasma membrane and promotes the invasion and movement of tumor cells^{8,9}. Moreover, mtp53 upregulates ENTPD5 expression to promote N-glycosylated membrane protein folding, eventually fostering lung metastasis¹⁰. Further research demonstrated that mtp53 variants promote metastasis via miRNA¹¹⁻¹³. Mtp53 protein has a new function of carcinogenesis and promoting cancer metastasis which depends on protein-protein interactions between mtp53 and other binding partners, including TFs such as Sp1 and ETS, and p53 family members such as p73 and p63¹⁴⁻¹⁸.

FRA-1 belongs to the activator protein 1 (AP-1) family and is considered as a critical mediator of EMT/MET balance in tumor cells¹⁹⁻²². It involves cell motility programs through its ability to control several genes encoding EMT-TFs (e.g., ZEB1, TWIST), cell-cell adhesion proteins (CD44), and extracellular matrix-degrading enzymes (MMP1, MMP9)²³⁻²⁷. FRA-1 is a hub, responding to various signals such as PKC θ /SPAK1, mTORC1/S6K1, and ERK²⁸⁻³¹. In this study, we identify mtp53 as a driver of FRA-1. We

analyzed the gene expression profile in metastatic BRAC cells to unravel the potential mechanism. We found a higher enrichment of FOSL1 (encoding FRA-1) in metastatic mutant p53 MDA-MB-231 cells than mutant p53 knockdown samples. In addition, we determined that FRA-1 expression depends on mtp53. In terms of mechanism, we discovered that mtp53 physically interacts with ELK-1 in MDA-MB-231 cells. Moreover, we disclosed that mtp53 and ELK-1 are recruited to the FOSL1 promoter together, suggesting they cooperate to induce FRA-1 expression. Additionally, in a comprehensive pan-cancer analysis, there was a highly significant correlation between FRA-1 expression and mutant p53.

In conclusion, this study highlights that FRA-1 is a novel target for mtp53 to promote cell migration, providing new insights into how mtp53 navigates the tumor metastasis process and opens up a new way for transformation therapy.

Materials And Methods

shRNA and generation of stable cells. MDA-MB-231, T47D, and 293T cells were purchased from ATCC. We generated lentiviruses (biosettia) with a single shRNA targeting p53 or Elk-1 (Table S1) to knock down p53 and Elk-1 in MDA-MB-231 and T47D cells. The infected MDA-MB-231 and T47D cells were selected using a medium supplemented with 10 mg/mL puromycin (Sigma Aldrich).

qRT-PCR and ChIP-qPCR. Total RNA was isolated with Trizol reagent (Invitrogen, USA). Then, the RNA (1 µg) was synthesized into cDNA using a reverse transcription kit (Qiagen). The ChIP-DNA was prepared using an anti-ELK-1 antibody in MDA-MB-231 as described. All gene expression data were normalized with an internal control gene (GADPH). All ChIP-qPCR data was normalized with target amplification site in input. Primer sequences were listed in Supplementary Table S2& Table S3.

Antibody. Antibodies were p53(#48818, Cell Signaling Technology), FRA-1(#5281, Cell Signaling Technology), ELK-1(#9182, Cell Signaling Technology), E-cadherin (#3195, Cell Signaling Technology), and β-actin (#4970, Cell Signaling Technology).

Immunofluorescent staining. Fix cells with 4% formaldehyde/PBS. After overnight incubation with anti-E-cadherin (1:200) at 4°C, the target protein was detected by anti-rabbit IgG PE-conjugated secondary antibody. Nuclei were stained with DAPI.

Wound-healing assay. Cells in 6-well plates were grown to confluence. Use a 200 ml pipette tip to draw a line from the monolayer to remove part of the cells. The area of migrated cells was estimated after 24 hours and analyzed with ImageJ software.

Transwell assay. For transwell migration assays, we seeded cells into the top chamber of a 24-well cell culture insert (Corning, 3422) with 1% FBS medium and then added 10% FBS medium to the bottom chamber. Cells transferred to the bottom of the membrane were fixed with 4% formaldehyde, stained with 0.05% crystal violet several hours later (MDA-MB-231, 17 hours; T47D, 45 hours), and counted. Measurements were performed in triplicates.

GSEA enrichment analysis. Gene Set Enrichment Analysis (GSEA) using the expression matrix of differential genes in control and Tp53 knockdown RNA-seq data, the selected reference gene sets were c2.cp.reactome.v7.5.1.symbols.gmt and c2.cp.kegg.v7.5.symbols.gmt. The ggplot2 package is used to visualize GSEA collections.

Analysis of TCGA gene expression data. To assess whether FRA-1 expression is induced in cancers with TP53 mutations, we used data from The Cancer Genome Atlas (TCGA). First, using XenaPython, we downloaded data from all samples in TCGA for BRCA, LUAD, and PAAD cancer types and classified the data, including wild-type p53 and p53GOF (missense mutations, including six hotspots ((R175, G245, R248, R249, R273, R282) together with R280K and L194F). GraphPad generated dot plots representing the distribution of gene expression values. Dot plots represent three genes in Tp53WT and Tp53GOF tumors from each cancer. The number of samples in each group was as follows: BRCA-p53WT = 675, Tp53GOF = 56; LUAD-p53WT = 276, Tp53GOF = 22; PAAD-p53WT = 57, Tp53GOF = 21.

Results

Mtp53 maintains EMT by enhancing the expression of a group of EMT-TFs

MDA-MB-231 cells are a classic cell model of TNBC, and their transformation phenotype depends on the high-level R280K mutant variant of p53. To better comprehend the potential mechanism of mtp53 GOF, we used a well-designed and previously published MDA-MB-231 expression profile analysis data set ³². Rather than examining one possible p53 gene at a time, GSEA analysis can identify sets of genes that represent molecular pathways and associated functions. GSEA analysis has demonstrated that the knockdown of p53 in the MDA-MB-231 cell line determines the EMT program. Among the gene groups, which are displaying the lowest NES value, are those associated with EMT. These include gene sets marked as KEGG pathway's ECM receptor interaction (NES= -1.555113), TGF- β signaling pathway (NES=-1.4465687), basal cell carcinoma (NES=-1.4356328), Reactome's degradation of the extracellular matrix (NES=-2.2472658), activation of matrix metalloproteinases (NES=-2.2133317), collagen degradation (NES=-2.133577), extracellular matrix organization (NES=-2.0230956), TGF- β receptor signaling in epithelial to mesenchymal transition (NES=-1.8143506), TGF- β receptor signaling activates SMADs (NES= -1.6533562) (Fig. 1A,B). The bulk mainly refers to the same genes essential for EMT transformation.

The GSEA analysis focused on EMT-related genes whose expression is reduced or induced upon EMT. Tissue inhibitor of metalloproteinase (TIMP-1, TIMP-2) is a natural inhibitor of matrix metalloproteinase (MMP). MMP increases after p53 gene knockout in MDA-MB-231 cells. In contrast, those mediate cell-to-cell and cell-to-matrix interactions molecular (THBS1, THBS2) reduced in p53 shRNA-expressing MDA-MB-231 cells. The reduction of mesenchymal genes, including VIM encoding vimentin, was also observed. Importantly, in response to mtp53 knockdown, a global decrease in a panel of EMT-TFs such as

SNAIL, ZEB1, ZEB2, YAP1, JUN was detected (Fig. 1C). Nevertheless, consistent with previous studies, our observations suggest that mtp53 is critical for maintaining EMT in BRAC.

Mtp53 endows cells with mesenchymal traits and promote FRA-1 expression

The GSEA analysis results show that mtp53 is involved in tumor invasion and metastasis. To examine this possibility, we investigated the mobility and transcriptional changes induced by mtp53 knockdown in MDA-MB-231 and T47D cells. To analyze the effect of mtp53 on cell migration, we performed wound-healing assays and transwell assays with MDA-MB-231 and T47D cells of mtp53 knockdown. From the results of these experiments, we can observe that mtp53 silencing decreases cell mobility (Fig. 2A). Immunofluorescence staining of MDA-MB-231 and T47D cells showed that cell-cell adhesion involving E-cadherin was induced upon mtp53 knockdown (Fig. 2B). These results indicated that mtp53 reduces the expression of E-cadherin and the formation of cell-cell adhesion, suggesting that mtp53 is essential for the maintenance of the mesenchymal characteristics of BRAC cells. Taken together, mtp53 is vital for cell mobility.

According to the heat map, we also observed an increase in FOSL1. Given the importance of FRA-1 in EMT balance, we would like to know whether mtp53 maintains EMT through FRA-1. To test this possibility, we studied the transcriptional changes of FRA-1 caused by mtp53 gene knockdown in MDA-MB-231 and T47D cells. As we estimated, knockdown of mtp53 with two independent shRNAs preferentially caused loss of FRA-1 (Fig. 2C, D). These results support the hypothesis that FRA-1 is vital to maintain the mesenchymal characteristics of cells harboring p53 mutations.

Mtp53 is a direct activator of FOSL1

Some of the mtp53 regulatory genes may be directly regulated by mtp53, while others may be indirectly regulated. To determine whether FOSL1 is directly controlled by mtp53, we leverage p53 ChIP-seq data to check whether mtp53 binds to FOSL1. 699 p53 DTGs identified in MDA-MB-231 cells were compared with the p53 direct target genes (DTGs) identified in A549 and HEPG2 cells. The results showed that 463 genes, including FOSL1, were shared by three cell lines (Fig. 3A). These data indicate that p53 target genes have little tissue specificity, and even artificial mutations occur in cells (HepG2 and A549).

Using MDA-MB-231 p53 ChIP-seq data³², we found that p53 binds to four regions of the intron of the FOSL1 locus, all of which harbor response elements that firmly match the consensus binding sequence of p53. It is worth noting that p53 binding is conserved in the p53 ChIP-seq dataset generated from A549 and HepG2, although p53 has only one binding site in HepG2 cells. We examined the genome-wide distribution of mtp53. Three representative mtp53 binding peaks were selected in the crucial range (Fig. 3B). ChIP-qPCR results confirm that mtp53 binds to the genomic region of FOSL1 in T47D cells and MDA-MB-231 (Fig. 3C). In conclusion, these data suggest that FOSL1 is a direct target of mtp53.

ELK1- mtp53 cooperation is required for FRA-1 Expression

The transcriptional function of *mtp53* is related to its interaction with other transcription factors, thereby interrupting or enhancing its target genes. Under certain conditions, *mtp53* can increase the activity of transcription factor partners, form transcription factor complexes with them, and be recruited to targeted promoters¹⁸. To elucidate the molecular mechanism by which p53 forms unique transcriptional complex factors in p53 mutant cells, we investigated the genome-wide distribution of other transcription factors using ChIP-seq data sets. Analyzing the synergy between p53 and other transcription factors will help to understand the characteristics of p53 synergy in specific cellular contexts.

Enhancers strongly regulate *FOSL1* transcription in its first intron, which contains some binding elements. Therefore, we manually searched UCSC for binding sites in the first intron of *FOSL1* with these published ChIP-seq data. It was found that a large number of TFs, such as ELK-1, JUN, and JUNB, were recruited to this region. Therefore, we chose ELK-1 for further analysis, with the highest clustering score of 1000 (total score of 1000). ELK-1 was recruited into active chromatin labeled by H3K27ac and H3K4me3 deposition (Fig. 4A) in HeLa-s3 cells, which was close to p53 occupation, highlighting the functional interaction between ELK-1 and p53. The region was also found in MCF-7 breast cancer cells, K562 leukemia cells, and GM12878 cells (not shown). Furthermore, co-immunoprecipitation (Co-IP) with p53 antibody from MDA-MB-231 cells and T47D cells revealed the interaction between *mtp53* and ELK-1 in both cell lines (Fig. 4B).

Knockdown experiments in MDA-MB-231 cells showed that ELK-1 made a significant contribution to *FOSL1* expression (Fig. 4C, D). A considerable contribution of ELK-1 to *FOSL1* expression was also inspected in T47D cells (Fig. 4C, D), suggesting that p53-ELK1 cooperation is usually crucial in p53 mutant cells.

FRA-1 Expression Levels Correlate with GOF *mtp53* in Human Tumor Samples

Tumor Genome Atlas (TCGA) RNA-sequencing data provided us with a novel approach to probe the correlation between TP53 GOF missense mutations and *FRA-1* expression. TP53 GOF missense mutations are prevalent in multiple cancer types. To test the effect of TP53 GOF on the downstream expression of *FRA-1* (compared with *SNAIL* and *SLUG*), we observed the expression of these genes in three types of cancer prevalent in the TP53 mutation: breast cancer (BRCA), lung adenocarcinoma (LUAD) and pancreatic cancer (PAAD).

We divided the cases into two classes for each cancer according to their p53 mutation status as wild-type p53 and p53GOF (missense mutation including R175, G245, R248, R249, R273, R282, R280K, and L194F). As Zhu pointed out in the study, other p53 mutations (other missense mutations, frame insertion/deletions, or splice mutations) and null p53 (p53 nonsense mutations or frameshift truncations) were not included in the further analysis because of significant differences in p53 function³³. The impact is unpredictable. Then, we compared the expression of *SNAIL*, *SLUG*, and *FRA-1* between the two classes in the three cancer types. Consistent with *mtp53*-dependent expression, *FRA-1* RNA levels were

significantly higher in cases with p53GOF mutations than wild-type p53 cases (Fig. 5). Similar but less robust patterns were observed for *SNAIL* and *SLUG* expression in both cases (Fig. 5). Thus, p53 GOF mutations are associated with high levels of *FRA-1* expression in a wide range of patient groups with different tumor entities.

Discussion

The prevalent TP53 mutations in human cancer have promoted the development of targeted therapy for the TP53 pathway³⁴. The realization of TP53-based treatment depends on a comprehensive understanding of the mechanism of tumor-related TP53 mutation. Through gene expression profiling of control & knockdown for Tp53 of MDA-MB-231 cells, we identified FOSL1 as a novel mediator of mtp53. We demonstrated for the first time that FOSL1 expression directly depended on mtp53, indicating that FRA-1 may be a novel mutant p53 effector. The comparative results of shRNA experiments in MDA-MB-231 and T47D cells showed that FRA-1 might be one of the crucial targets of mtp53 in BRAC. We demonstrated that mtp53 interacted directly with ELK-1 and their synergistic effect induces FOSL1 gene expression. High levels of FRA-1 expression are associated with p53GOF mutations in multiple tumors, which may underlie a possible basis for common cancer metastasis.

This study regarded FRA-1 as a novel downstream effector of mutated p53 that favored tumor metastasis. FRA-1 establishes and maintains the EMT program in different cancer types by directly regulating the expression of EMT-TFs²². In breast epithelial cells, RAS / ERK2 increases the expression of ZEB1 and ZEB2 by driving FRA-1 upregulation, resulting in complete EMT³⁵. In malignant melanoma cells, it is shown that FRA-1 binds directly to AP-1 binding elements located in *TWIST1*, *SNAIL2*, *ZEB1*, and *ZEB2* gene promoters²⁷. The Weinberg lab's findings reinforce the central role of FRA-1 in EMT. FOSL1 is directly motivated by TWIST1 and SNAIL1, thereby acting as an effector of the EMT pathway³⁶. Furthermore, FOSL1 serves as a hub that brings together numerous upstream regulatory pathways, including oncogenes of the MEK-ERK module and tumor suppressors such as p53, APC, and PTEN²².

Here, we illustrated that mtp53 interacted with ELK-1 and regulated FRA-1 expression by binding to the FOSL1 promoter, ultimately promoting tumor metastasis. The control role of ELK-1 on the migration of several human breast cells has been demonstrated, suggesting that ELK-1 plays a part in the metastasis of breast cancer cells³⁷. Genome-wide analysis showed that most of the genes targeted by ELK-1 were related to cell migration and actin cytoskeleton³⁸. In addition, ELK-1 was recruited to the ETS binding site of the MMP-9 promoter, thus enhancing its transcription³⁹. There are many TFs occupied on the promoter of FOSL1, including ELK-1, SRF, AP-1, and ATF/CREB³⁵. Although we cannot formally exclude additional partners of mtp53, ELK-1 may be a significant recruitment factor because the consumption of ELK-1 impairs FRA-1 expression in BRAC.

In light of the role of FRA-1 in metastasis, targeting FRA-1 in aggressive BRCA may be a new therapeutic option. This study offers a prism through which to look at the molecular basis of mtp53-driven

metastasis and an identification scheme for a novel p53 mutational metastatic therapeutic target.

Declarations

Data availability

The datasets analyzed during the current study are available as follows. Gene expression microarray data can be accessed under GEO Accession No. GSE68248. ChIP-seq data were obtained from GEO Accession No. GSE66543 (MDA-MB-231) and ENCODE Project Consortium: A549 (ENCSR112XUO), HepG2 (ENCSR980EGJ), and Hela-s3 (ENCSR454DOC, ENCSR717QSS, ENCSR068MRQ).

Author contributions

S.H. and H.L. designed the experiments, performed the statistical analysis, and wrote the manuscript. M.W., A. J., J.Y., R. G., X.L., and L.S performed experiments acquired. Z.Y. and Y.Z. assisted with writing the manuscript. All authors reviewed and approved the final version of the manuscript.

Competing interests

The authors declare no competing interests.

References

1. Kandoth, C.*et al.* Mutational landscape and significance across 12 major cancer types. *Nature* **502**, 333-339, doi:10.1038/nature12634 (2013).
2. Rivlin, N., Brosh, R., Oren, M. & Rotter, V. Mutations in the p53 Tumor Suppressor Gene: Important Milestones at the Various Steps of Tumorigenesis. *Genes Cancer* **2**, 466-474, doi:10.1177/1947601911408889 (2011).
3. Tang, Q., Su, Z., Gu, W. & Rustgi, A. K. Mutant p53 on the Path to Metastasis. *Trends Cancer* **6**, 62-73, doi:10.1016/j.trecan.2019.11.004 (2020).
4. Dong, P.*et al.* Mutant p53 gain-of-function induces epithelial-mesenchymal transition through modulation of the miR-130b-ZEB1 axis. *Oncogene* **32**, 3286-3295, doi:10.1038/onc.2012.334 (2013).
5. Roger, L., Jullien, L., Gire, V. & Roux, P. Gain of oncogenic function of p53 mutants regulates E-cadherin expression uncoupled from cell invasion in colon cancer cells. *J Cell Sci* **123**, 1295-1305, doi:10.1242/jcs.061002 (2010).
6. Ohashi, S.*et al.* Epidermal growth factor receptor and mutant p53 expand an esophageal cellular subpopulation capable of epithelial-to-mesenchymal transition through ZEB transcription factors. *Cancer Res* **70**, 4174-4184, doi:10.1158/0008-5472.CAN-09-4614 (2010).
7. Adisheshaiah, P., Papaiahgari, S. R., Vuong, H., Kalvakolanu, D. V. & Reddy, S. P. Multiple cis-elements mediate the transcriptional activation of human fra-1 by 12-O-tetradecanoylphorbol-13-acetate in bronchial epithelial cells. *J Biol Chem* **278**, 47423-47433, doi:10.1074/jbc.M303505200 (2003).

8. Muller, P. A.*et al.* Mutant p53 drives invasion by promoting integrin recycling. *Cell* **139**, 1327-1341, doi:10.1016/j.cell.2009.11.026 (2009).
9. Caswell, P. & Norman, J. Endocytic transport of integrins during cell migration and invasion. *Trends Cell Biol* **18**, 257-263, doi:10.1016/j.tcb.2008.03.004 (2008).
10. Vogiatzi, F.*et al.* Mutant p53 promotes tumor progression and metastasis by the endoplasmic reticulum UDPase ENTPD5. *Proc Natl Acad Sci U S A* **113**, E8433-E8442, doi:10.1073/pnas.1612711114 (2016).
11. Novo, D.*et al.* Mutant p53s generate pro-invasive niches by influencing exosome podocalyxin levels. *Nat Commun* **9**, 5069, doi:10.1038/s41467-018-07339-y (2018).
12. Cooks, T.*et al.* Mutant p53 cancers reprogram macrophages to tumor supporting macrophages via exosomal miR-1246. *Nat Commun* **9**, 771, doi:10.1038/s41467-018-03224-w (2018).
13. Subramanian, M.*et al.* A mutant p53/let-7i-axis-regulated gene network drives cell migration, invasion and metastasis. *Oncogene* **34**, 1094-1104, doi:10.1038/onc.2014.46 (2015).
14. Freed-Pastor, W. A. & Prives, C. Mutant p53: one name, many proteins. *Genes Dev* **26**, 1268-1286, doi:10.1101/gad.190678.112 (2012).
15. Kim, M. P. & Lozano, G. Mutant p53 partners in crime. *Cell Death Differ* **25**, 161-168, doi:10.1038/cdd.2017.185 (2018).
16. Melino, G. p63 is a suppressor of tumorigenesis and metastasis interacting with mutant p53. *Cell Death Differ* **18**, 1487-1499, doi:10.1038/cdd.2011.81 (2011).
17. Chicas, A., Molina, P. & Bargonetti, J. Mutant p53 forms a complex with Sp1 on HIV-LTR DNA. *Biochem Biophys Res Commun* **279**, 383-390, doi:10.1006/bbrc.2000.3965 (2000).
18. Muller, P. A. & Vousden, K. H. p53 mutations in cancer. *Nat Cell Biol* **15**, 2-8, doi:10.1038/ncb2641 (2013).
19. Lloyd, A., Yancheva, N. & Wasylyk, B. Transformation suppressor activity of a Jun transcription factor lacking its activation domain. *Nature* **352**, 635-638, doi:10.1038/352635a0 (1991).
20. Tulchinsky, E. Fos family members: regulation, structure and role in oncogenic transformation. *Histol Histopathol* **15**, 921-928, doi:10.14670/HH-15.921 (2000).
21. Ransone, L. J. & Verma, I. M. Nuclear proto-oncogenes fos and jun. *Annu Rev Cell Biol* **6**, 539-557, doi:10.1146/annurev.cb.06.110190.002543 (1990).
22. Dhillon, A. S. & Tulchinsky, E. FRA-1 as a driver of tumour heterogeneity: a nexus between oncogenes and embryonic signalling pathways in cancer. *Oncogene* **34**, 4421-4428, doi:10.1038/onc.2014.374 (2015).
23. Belguise, K., Kersual, N., Galtier, F. & Chalbos, D. FRA-1 expression level regulates proliferation and invasiveness of breast cancer cells. *Oncogene* **24**, 1434-1444, doi:10.1038/sj.onc.1208312 (2005).
24. Ramos-Nino, M. E., Scapoli, L., Martinelli, M., Land, S. & Mossman, B. T. Microarray analysis and RNA silencing link fra-1 to cd44 and c-met expression in mesothelioma. *Cancer Res* **63**, 3539-3545 (2003).

25. Zhao, C.*et al.* Genome-wide profiling of AP-1-regulated transcription provides insights into the invasiveness of triple-negative breast cancer. *Cancer Res* **74**, 3983-3994, doi:10.1158/0008-5472.CAN-13-3396 (2014).
26. Diesch, J.*et al.* Widespread FRA1-dependent control of mesenchymal transdifferentiation programs in colorectal cancer cells. *PLoS One* **9**, e88950, doi:10.1371/journal.pone.0088950 (2014).
27. Caramel, J.*et al.* A switch in the expression of embryonic EMT-inducers drives the development of malignant melanoma. *Cancer Cell* **24**, 466-480, doi:10.1016/j.ccr.2013.08.018 (2013).
28. Belguise, K.*et al.* The PKC θ pathway participates in the aberrant accumulation of Fra-1 protein in invasive ER-negative breast cancer cells. *Oncogene* **31**, 4889-4897, doi:10.1038/onc.2011.659 (2012).
29. Pakay, J. L.*et al.* A 19S proteasomal subunit cooperates with an ERK MAPK-regulated degron to regulate accumulation of Fra-1 in tumour cells. *Oncogene* **31**, 1817-1824, doi:10.1038/onc.2011.375 (2012).
30. Vial, E. & Marshall, C. J. Elevated ERK-MAP kinase activity protects the FOS family member FRA-1 against proteasomal degradation in colon carcinoma cells. *J Cell Sci* **116**, 4957-4963, doi:10.1242/jcs.00812 (2003).
31. Gu, X.*et al.* Integration of mTOR and estrogen-ERK2 signaling in lymphangioliomyomatosis pathogenesis. *Proc Natl Acad Sci U S A* **110**, 14960-14965, doi:10.1073/pnas.1309110110 (2013).
32. Walerych, D.*et al.* Proteasome machinery is instrumental in a common gain-of-function program of the p53 missense mutants in cancer. *Nat Cell Biol* **18**, 897-909, doi:10.1038/ncb3380 (2016).
33. Zhu, J.*et al.* Gain-of-function p53 mutants co-opt chromatin pathways to drive cancer growth. *Nature* **525**, 206-211, doi:10.1038/nature15251 (2015).
34. Lane, D. P., Cheek, C. F. & Lain, S. p53-based cancer therapy. *Cold Spring Harb Perspect Biol* **2**, a001222, doi:10.1101/cshperspect.a001222 (2010).
35. Young, M. R. & Colburn, N. H. Fra-1 a target for cancer prevention or intervention. *Gene* **379**, 1-11, doi:10.1016/j.gene.2006.05.001 (2006).
36. Tam, W. L.*et al.* Protein kinase C alpha is a central signaling node and therapeutic target for breast cancer stem cells. *Cancer Cell* **24**, 347-364, doi:10.1016/j.ccr.2013.08.005 (2013).
37. Odrowaz, Z. & Sharrocks, A. D. The ETS transcription factors ELK1 and GABPA regulate different gene networks to control MCF10A breast epithelial cell migration. *PLoS One* **7**, e49892, doi:10.1371/journal.pone.0049892 (2012).
38. Odrowaz, Z. & Sharrocks, A. D. ELK1 uses different DNA binding modes to regulate functionally distinct classes of target genes. *PLoS Genet* **8**, e1002694, doi:10.1371/journal.pgen.1002694 (2012).
39. Hsieh, H. L., Wu, C. Y. & Yang, C. M. Bradykinin induces matrix metalloproteinase-9 expression and cell migration through a PKC- δ -dependent ERK/Elk-1 pathway in astrocytes. *Glia* **56**, 619-632, doi:10.1002/glia.20637 (2008).

Figures

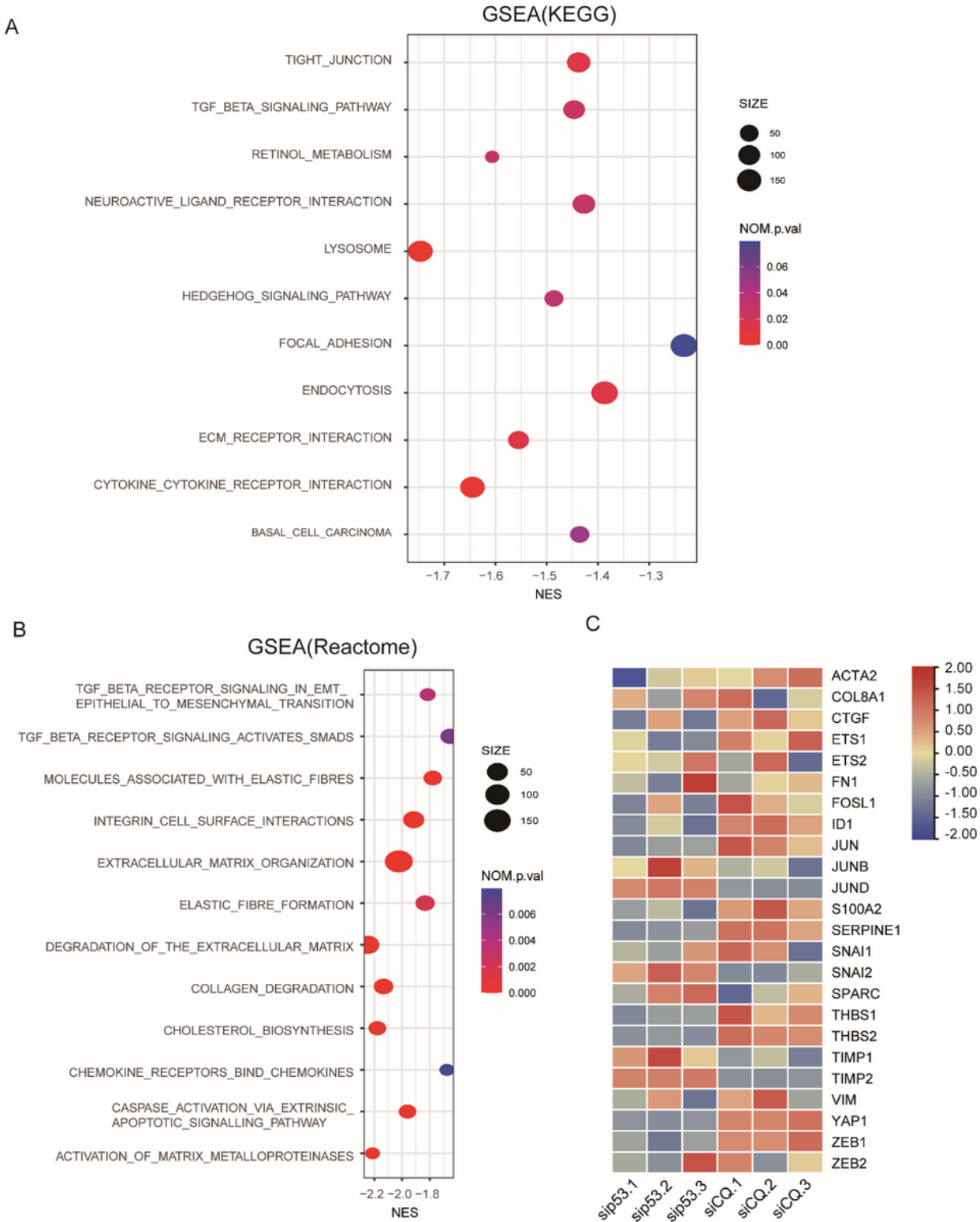
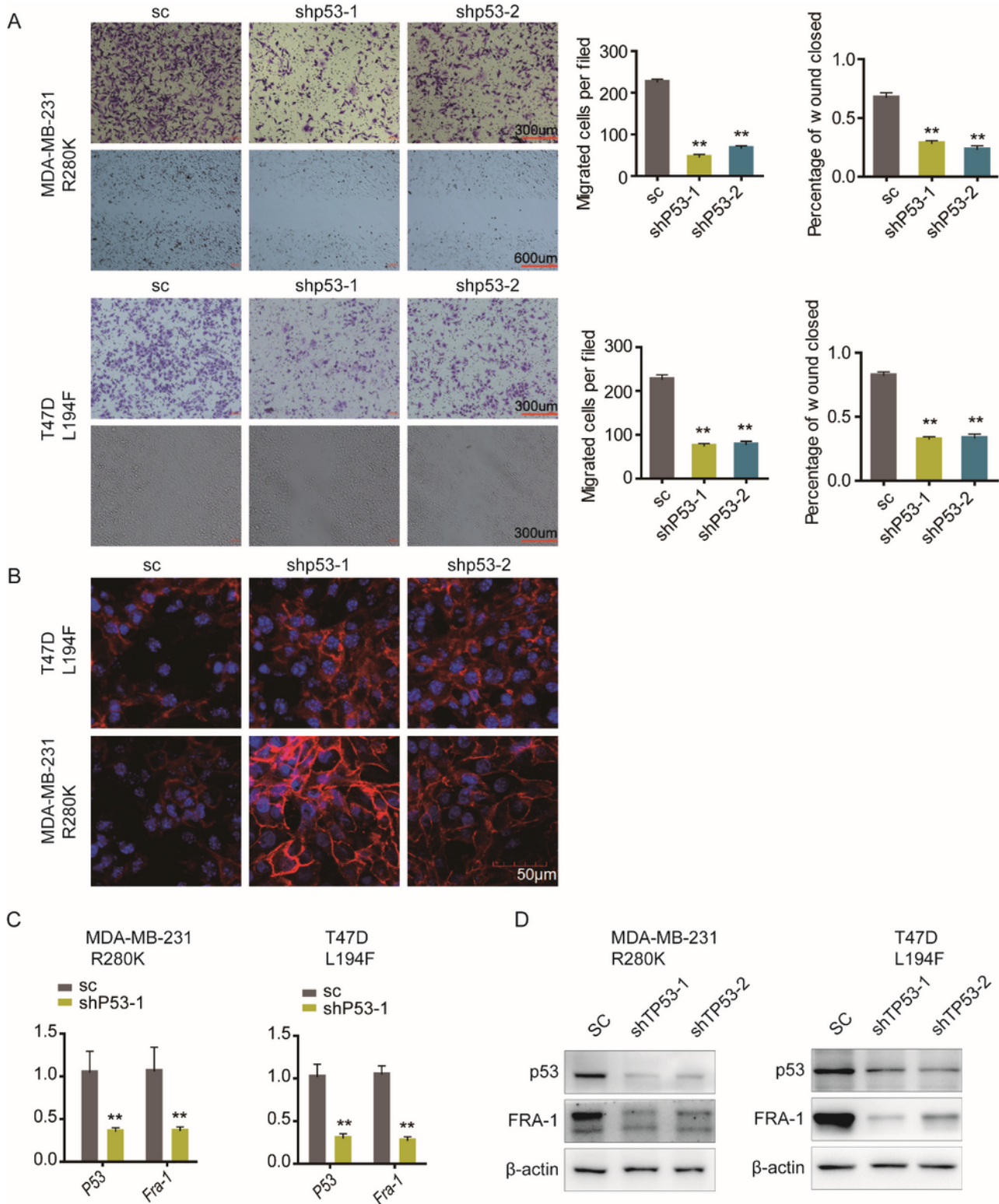


Figure 1

Pathway and gene identified through GSEA. Bubble chart of KEGG enrichment (A) and Reactome enrichment (B) analysis on gse68249 dataset using GSEA. The bubble color changes from blue to red, indicating a gradual increase in significance. Heatmap shows the RNA sequencing results of arbitrarily

selected EMT-related genes in MDA-MB-231(C), ignoring P value and fold change. Counts were normalized by Deseq2 (GSE68249).



from student t-test, $**p \leq 0.01$; $*p \leq 0.05$ Immunofluorescence staining of E-cadherin in mtp53-silenced MDA-MB-231 and T47D cells (B). Scale bar, 50um. QRT-PCR analyses of the indicated transcripts (relative to GADPH)(C). mRNA expression is normalized to the expression of control cells. All data are presented as mean \pm SD, $**p \leq 0.01$; $*p \leq 0.05$. Immunoblot analysis of FRA-1 in mtp53-silenced MDA-MB-231 and T47D cells (D).

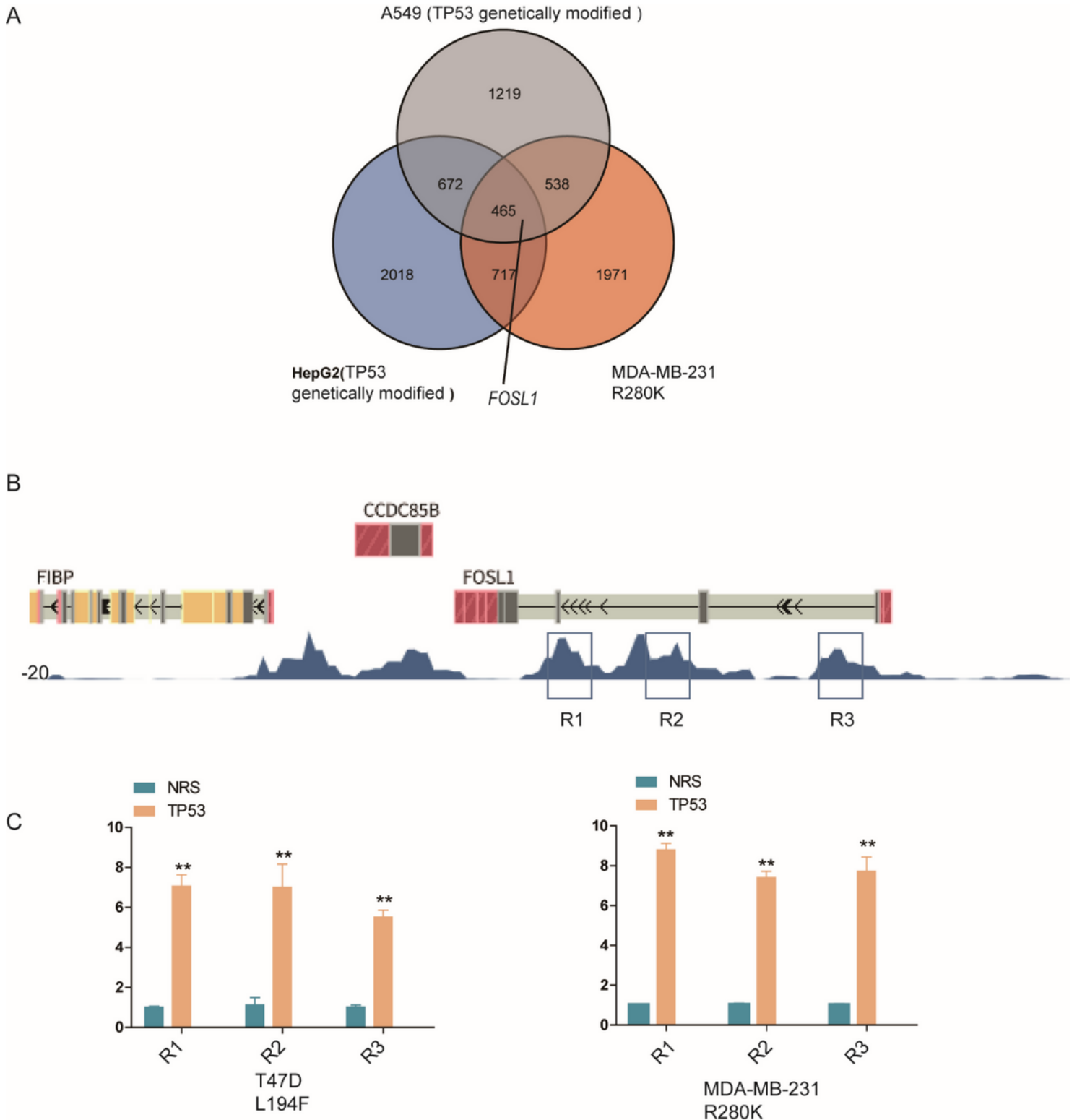


Figure 3

TP53 directly controls FOSL1. Comparison of mtp53 DTGs in three cancer cell lines from different tissues. Venn diagram shows the number of mtp53 DTGs identified in HepG2, A549, and MDA-MB-231 cells (A). The numbers in the pie chart overlap represent shared genes. FOSL1 is shared among three cancer cell lines.

(B)ChIP-seq binding profile of mtp53 in A549. (C) ChIP-qPCR analysis of TP53 in MDA-MB-231 and T47D cells. Relative fold changes were normalized to normal rabbit serum (NRS). All data were expressed as mean \pm SD. ** $p \leq 0.01$; * $p \leq 0.05$

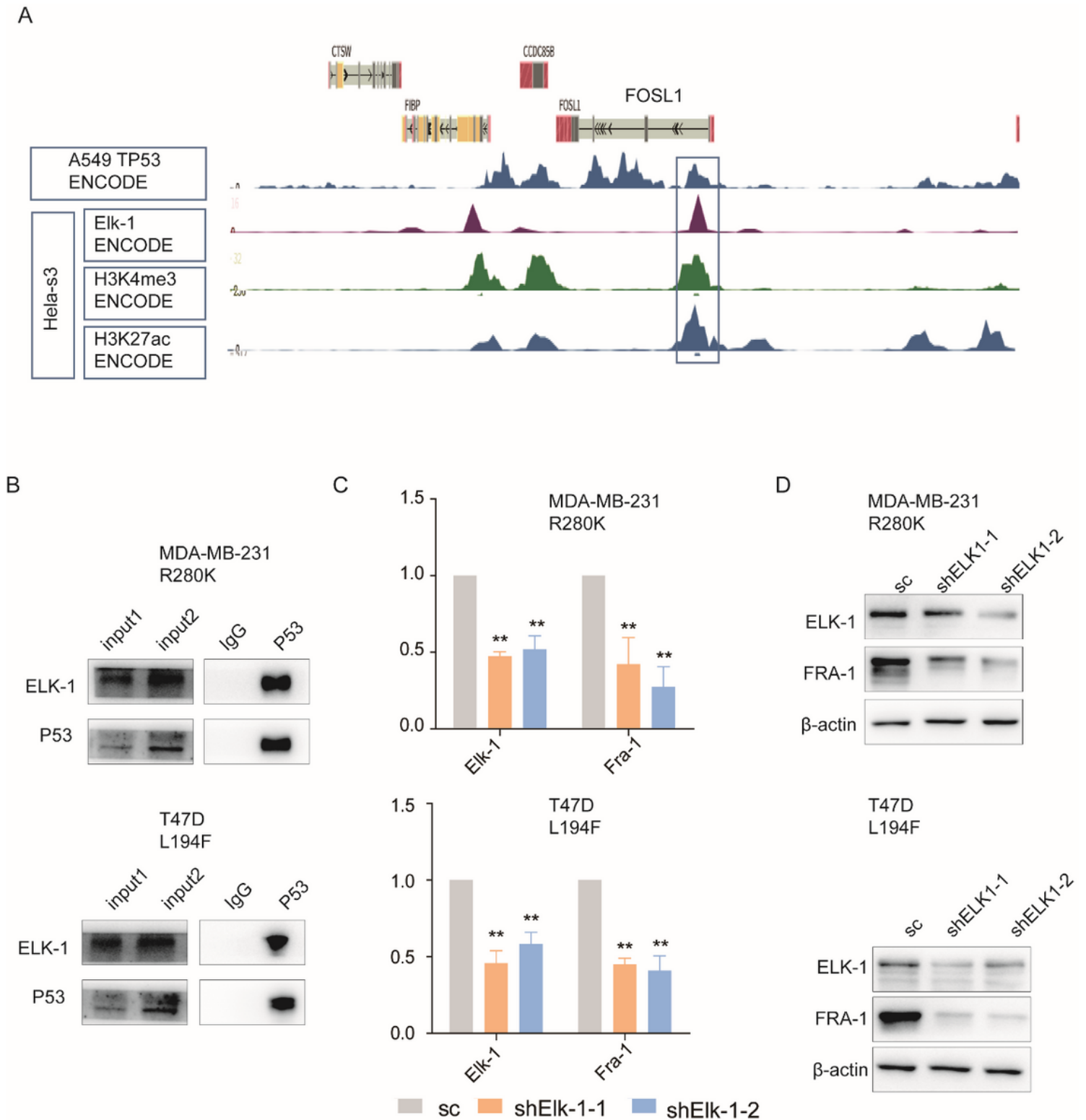


Figure 4

ELK-1 acts as a cofactor of mtp53. ChIP-seq profile of the FOSL1 locus. P53 chromatin binding in A549 cells, ELK-1 chromatin binding, H3K27ac& H3K4me3 deposition patterns in HeLa-s3 cells were obtained from the ENCODE database (A). The protein extracts of MDA-MB-231 and T47D cells were immunoprecipitated (IP) with IgG or p53 antibody, and then p53 and ELK-1 were immunoblotted (B). Q-PCR analyzed the indicated transcripts (relative to GADPH) on ELK-1 knockdown in MDA-MB-231 and

T47D cells(C). All data are expressed as mean \pm SD. ** $p \leq 0.01$; * $p \leq 0.05$. Elk-1 and FRA-1 were detected by Western blot analysis on ELK-1 knockdown in MDA-MB-231 and T47D cells (D).

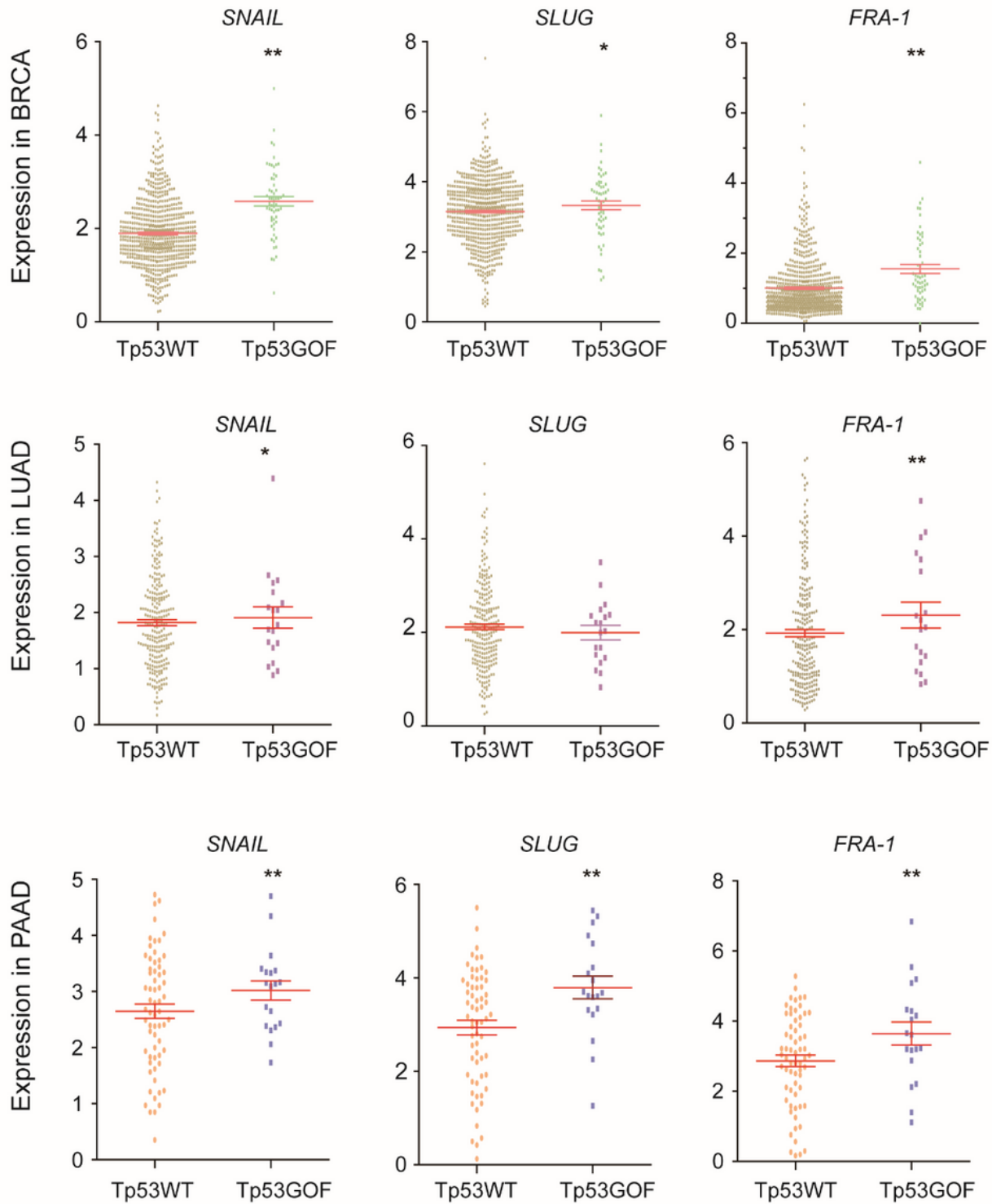


Figure 5

FRA-1 induction in tumors with P53 mutations. The gene expression values of SNAIL, SLUG, and FRA-1 in breast cancer (BRCA), lung adenocarcinoma (LUAD), and pancreatic cancer (PAAD). Expression values

were based on Pan-cancer standardized RNA-seq data from The Cancer Genome Atlas (TCGA). Each point represents the expression level of a single tumor, and the horizontal line stands for the average expression of cancer/genotype population. Significant changes in Tp53GOF relative to Tp53WT are shown (Wilcoxon rank-sum test; ** $p \leq 0.01$; * $p \leq 0.05$).

Supplementary Files

This is a list of supplementary files associated with this preprint. Click to download.

- [supplementary.docx](#)